New band structures and an unpaired crossing in ^{78}Kr

H. Sun,[1,*] J. Döring,[1,2] G. D. Johns,[1,†] R. A. Kaye,[1,‡] G. Z. Solomon,[1] S. L. Tabor,[1] M. Devlin,[3] D. R. LaFosse,[3] F. Lerma,[3] D. G. Sarantites,[3] C. Baktash,[4] D. Rudolph,[4,§] C.-H. Yu,[4] I. Y. Lee,[5] A. O. Macchiavelli,[5] I. Birriel,[6] J. X. Saladin,[6] D. F. Winchell,[6] V. Q. Wood,[6] and I. Ragnarsson[7]

[1]*Department of Physics, Florida State University, Tallahassee, Florida 32306*
[2]*Department of Physics, University of Notre Dame, Notre Dame, Indiana 46556*
[3]*Department of Chemistry, Washington University, St. Louis, Missouri 63130*
[4]*Physics Division, Oak Ridge National Laboratory, Oak Ridge, Tennessee 37831*
[5]*Nuclear Science Division, Lawrence Berkeley National Laboratory, Berkeley, California 94720*
[6]*Department of Physics and Astronomy, University of Pittsburgh, Pittsburgh, Pennsylvania 15260*
[7]*Department of Mathematical Physics, Lund Institute of Technology, S-22100 Lund, Sweden*

(Received 6 July 1998)

High-spin states in ^{78}Kr were studied using the ^{58}Ni(^{23}Na,3p) reaction at 70 MeV and the ^{58}Ni(^{28}Si,$\alpha 4p$) reaction at 130 MeV. Prompt γ-γ coincidences were measured using the Pitt-FSU detector array and the GAMMASPHERE-MICROBALL array. Results from these experiments have led to 26 new excitation levels, some of which have been grouped into 3 new bands. Spins were assigned based on directional correlations of oriented nuclei. Two of the new negative-parity bands appear to form a signature-partner pair based on a two-quasineutron structure, in contrast to the previously known two-quasiproton negative-parity bands. A forking has been observed at the 24^+ state in the yrast band, which calculations suggest may result from an unpaired crossing. The available evidence suggests oblate shapes in the yrast band coexist with prolate shapes in the negative-parity bands. [S0556-2813(99)04602-6]

PACS number(s): 21.10.Re, 21.60.Ev, 23.20.Lv, 27.50.+e

I. INTRODUCTION

The high-spin states of many even-even Kr isotopes have recently been of considerable theoretical and experimental interest. This interest is due to their rich variety of shapes, with particular nuclei exhibiting shape coexistence. Quadrupole deformations vary rapidly with N, ranging from the highly deformed ^{74}Kr($\beta_2 \approx 0.37$) [1–3] to the weakly deformed ^{82}Kr($\beta_2 \approx 0.15$) [4]. Various models have been used to study the ground-state deformation and the evolution of shape, including the interacting boson model [5], the two-quasiparticle-plus-rotor model [6], the cranked Hartree-Fock-Bogoliubov model with a Woods-Saxon potential [7,8], and the deformed configuration-mixing shell model [9]. When these models are applied to ^{78}Kr, a large quadrupole deformation is calculated, in reasonable agreement with the experimental data, and near-oblate shapes compete with prolate ones.

In-beam γ-ray spectroscopy of ^{78}Kr has been performed with several fusion-evaporation reactions induced by ^{4}He, ^{12}C, ^{16}O, ^{18}O, and ^{24}Mg projectiles [5,7,10–13]. A positive-parity yrast band reaching up to spin 14^+ at 6480 keV, a positive-parity γ band and negative-parity yrast bands (spins up to 13^-) were established in Ref. [5] and extended to higher spin values in Refs. [7,12]. Many works mentioned above explained the first band crossing in the yrast band of ^{78}Kr in terms of the alignment of a pair of $g_{9/2}$ protons. However, the g factor measured [14] for the 8^+ state (and states just above this) was found to be less than the collective value, indicating that the aligning nucleons at the lowest band crossing are $g_{9/2}$ neutrons, instead.

A major purpose of the present experiments was to search for new negative-parity bands similar to those which have been reported in ^{76}Kr [15] and ^{80}Kr [16]. Only one pair of negative-parity bands, believed to be predominately two-quasiproton in nature, was previously known in ^{78}Kr. Since somewhat analogous two-quasineutron bands had recently been found in ^{76}Kr, the question arose whether such structures could be found in ^{78}Kr. The higher spins accessible with the new detector arrays also lead to the possibility of observing effects of the microscopic structure underlying collective bands.

II. EXPERIMENTAL PROCEDURE

Two reactions were used to populate high-spin states in ^{78}Kr. The first was the ^{58}Ni(^{23}Na,3p) reaction at 70 MeV. The beam was provided by the Florida State University Tandem-LINAC facility. The ^{58}Ni target was 19.44 mg/cm^2 thick and isotopically enriched to 99.89%. The γ rays were detected with the Pitt-FSU detector array [17] consisting of 10 Compton-suppressed high-purity Ge detectors. A total of approximately 1.5×10^7 events was collected and sorted [18] into two triangular matrices with dispersions of 0.5 keV/channel and 1.0 keV/channel with all possible detector pairs and a square matrix with a dispersion of 0.8 keV/channel

*Permanent address: Department of Physics, Jilin University, Changchun, Jilin 130023, People's Republic of China.
†Present address: Los Alamos National Laboratory, Los Alamos, NM 87545.
‡Present address: Physics Division, Argonne National Laboratory, Argonne, IL 60439.
§Present address: Department of Physics, Lund University, S-22100 Lund, Sweden.

containing coincidences between the 35° and 145° detectors on one axis and the 90° detectors on the other. Background-subtracted gated spectra projected from the triangular matrix yielded the γ-ray energies and intensities. A similar energy gating technique used on the square matrix yielded directional correlation of oriented nuclei (DCO) ratios.

The second reaction was ^{58}Ni(^{28}Si,$\alpha 4p$) at 130 MeV. The beam was provided by the 88-in. cyclotron at Lawrence Berkeley National Laboratory, and the target, enriched to 99.7% in ^{58}Ni, was 330 μg/cm^2 thick. The GAMMASPHERE array [19] consisting of 57 high-efficiency Ge detectors at the time was used to collect prompt coincidence events. The 95-element MICROBALL charged-particle detector array [20] provided channel selection and information to kinematically reconstruct each event to substantially reduce Doppler broadening. Approximately 5×10^6 triples and higher fold events were recorded on tape for the α-4p evaporation channel. Several triangular matrices were constructed by gating on α-4p events and combinations of γ transitions in the various bands.

Spins were assigned based on DCO ratio measurements. The DCO ratios were determined from the FSU data according to

$$R_{\mathrm{DCO}}=\frac{I_\gamma(\text{at } \theta \text{ gated by } \gamma_{\mathrm{G}} \text{ at } 90^\circ)}{I_\gamma(\text{at } 90^\circ \text{ gated by } \gamma_{\mathrm{G}} \text{ at } \theta)}, \qquad (1)$$

where θ was 35° or 145°. The gate γ_{G} was set on one or more stretched electric quadrupole ($E2$) transitions. The DCO ratios for stretched $E2$ transitions as well as for pure dipole $\Delta I=0$ transitions are expected to be approximately unity, while stretched $\Delta I=1$ transitions yield ratios of about 0.5 if the multipole mixing ratio is small [21]. The DCO ratios measured, along with level energies, spins, and relative intensities are given in Table I.

III. LEVEL SCHEME

The present level scheme, shown in Fig. 1, was deduced from coincidence spectra generated by gating on the triangular γ-γ matrices and γ-gated triples matrices. Altogether, over 60 new transitions were identified, leading to 26 new excited states. Arbitrary numbers are placed above the bands in Fig. 1 to facilitate the discussion.

A. Positive-parity bands 1 and 2

The positive-parity odd-spin sequence, band 2, was known [7] up to the (9^+) level at 4251 keV. In our work, two higher transitions of 1188 and 1391 keV were identified, leading to a tentative (13^+) level. Band 1 is an even-spin sequence which was previously identified [7] up to a tentative (10^+) level. We could not confirm the last tentatively placed 1088 keV $(10^+)\rightarrow(8^+)$ transition in our coincidence data. Instead two transitions of 1087 and 1088 keV have been placed in bands 4 and 6. One additional interband transition of 427 keV between band 2 and band 1 has been found in our work.

B. Positive-parity yrast band 3

The yrast band of ^{78}Kr was previously observed to a tentative 15 160 keV (24^+) state [7]. The present work confirms this structure and provides additional spin assignments in the band. Three new lines at 2040, 2098, and 2133 keV were observed in coincidence with the transitions in band 3, as shown in Fig. 2. Their energy relations strongly suggest the forking arrangement shown in Fig. 1. It was not possible to verify the ordering of the 2040 and 2098 keV transitions because of lack of statistics. Therefore, these transitions and the corresponding new level are shown with dashed lines.

C. New negative-parity bands 4–6

A new band was observed in both the FSU and GAMMASPHERE data. It is built on a new (4^-) level at 2891 keV. This level depopulates mainly by a 1326 keV γ ray to the 3^+ state at 1565 keV. The next band member, the (6^-) 3341 keV level, deexcites by four transitions (269, 276, 450, and 592 keV), where the 450 keV transition is weak in intensity and near the very strong 455 keV ground state transition. The 276 keV transition is contaminated by lines from ^{78}Rb [22], ^{77}Kr [23], and ^{78}Sr [24], but a gate on the 873 keV transition identifies it very clearly, as seen in Fig. 3. The 276 and 592 keV decays to known 5^- states [25] suggest negative parity for this band. Although the DCO ratios of the 276, 873, and 1004 keV lines provide spin assignments to three states in this band, we have left all the spins and parities in parentheses due to the weakness of the lines and possible contamination of the 276 keV transition. This non-yrast band was observed up to a tentative (14^-) state. Although a 1087 keV line was previously associated with the decay of the 5_2^- state [25], the coincidence relations and relative intensities strongly support a 1088 keV transition near the top of band 6, as shown in Fig. 1.

Band 5 is built on the previously known state at 3704 keV [11,13], which decays by a 1726 keV transition to the yrast band. A portion of the γ spectrum in coincidence with two gates in this band is shown in Fig. 4. The DCO ratio of the 1726 keV transition (Table I) and an earlier angular distribution measurement [13] provide a spin assignment of $7\hbar$ to this state. Similarly, the DCO ratios of the 969 and 1679 keV decay lines provide a spin assignment of 9 to the next state in the band. The parity of band 5 cannot be determined with certainty from the observed decay branches. However, the 269 and 509 keV decays from band 6 to 5 suggest negative parity for band 5. These decays and the excitation energy of this band suggest also that it is the signature partner of band 6. The previously known 3072 keV (5^-) level has been placed in this band because of a newly observed 632 keV decay to it. However, as in other nearby even-even nuclei, there is evidence of mixing among the low-lying negative-parity levels and band assignments in this region may not be completely unique.

Two new states at 4732 and 5838 keV were observed which decay by a cascade to a previously known (7^-) level at 3771 keV. They appear to form another band of probably negative parity—band 4. A previously known 5^- state at 3065 keV has been placed below band 4 in the level scheme, although no connecting transition has been observed, because it is involved in the negative-parity decay scheme.

TABLE I. Energies, initial and final spin states, relative intensities, and DCO ratios for observed transitions in ^{78}Kr.

E_x(keV)[a]	E_γ(keV)	$I_i^\pi(\hbar)$	$I_f^\pi(\hbar)$	I_γ[b]	R_{DCO}[b,c]
		Band 1			
1147.8	692.9(3)	2^+	2^+	9.5(6)	1.01(8)
	1147.8(3)	2^+	0^+	4.4(5)	1.00(4)
1872.6	724.8(3)	4^+	2^+	7.0(3)	0.99(7)
	753.2(7)	4^+	4^+	2.1(5)	0.87(24)
	1417.4(7)	4^+	2^+	1.2(3)	
2731.5	753(1)	6^+	6^+	0.8(3)	0.75(24)
	858.9(7)	6^+	4^+	2.4(4)	1.01(20)
3770.7	1039.2(6)	8^+	6^+	0.9(3)	1.1(3)
		Band 2			
1564.7	417.1(3)	3^+	2^+	3.9(7)	0.71(22)
	1109.8(2)	3^+	2^+	9.2(7)	0.68(18)
2299.8	426.5(4)[d]	5^+	4^+	3.5(4)	0.59(21)
	735.1(3)	5^+	3^+	7.9(7)	1.17(15)
	1180.3(4)	5^+	4^+	2.3(5)	0.72(21)
3202.7	902.9(4)	7^+	5^+	2.1(15)	1.04(7)
4253.7	1051.0(4)	9^+	7^+	0.7(1)	0.82(15)
5442[d]	1188(1)[d]	(11^+)	9^+	$\approx$0.2	
(6833)[d]	(1391)[d]	(13^+)	(11^+)	$\approx$0.2	
		Band 3			
454.9	454.9(1)	2^+	0^+	100[e]	1.05(7)
1119.4	664.5(2)	4^+	2^+	70(2)	1.02(7)
1977.6	858.4(2)	6^+	4^+	42(2)	0.96(9)
2993.5	1015.7(3)	8^+	6^+	24(2)	1.06(11)
4105.8	1112.2(3)	10^+	8^+	$\approx$9.0	1.1(1)[f]
5217.4	1112.2(5)	12^+	10^+	$\approx$6.0	1.1(1)[f]
6479.4	1262.2(4)	14^+	12^+	2.7(11)	1.04(8)
7936.4	1456.8(5)	16^+	14^+	1.4(8)	0.9(4)
9568	1632(1)	(18^+)	16^+	1.5(8)	
11312	1744(1)	(20^+)	(18^+)	1.3(7)	
13157	1845(1)	(22^+)	(20^+)	0.9(3)	
15160	2003(1)	(24^+)	(22^+)	0.7(3)	
(15197)[d]	(2040)[d]	(24^+)	(22^+)	$\approx$0.4	
(17293)[d]	(2098)[d]	(26^+)	(24^+)	$\approx$0.3	
	(2133)[d]	(26^+)	(24^+)	$\approx$0.5	
		Band 4			
3065.0	315(1)[d]	5^-	5^-	1.0(4)	0.89(15)
	(765)[d]	5^-	5^+	0.3(1)	
	1087.4(5)	5^-	6^+	1.1(4)	
3770.8	698.9(4)[d]	(7^-)	(5^-)	$\approx$0.3	
	1793.6(6)	(7^-)	6^+	1.6(3)	
4731.5[d]	960.7(6)[d]	(9^-)	(7^-)	$\approx$0.2	
5838[d]	1106(1)[d]	(11^-)	(9^-)	$\approx$0.1	
		Band 5			
3071.6	1199.4(5)[d]	(5^-)	4^+	0.6(2)	
	1952.2(6)	(5^-)	4^+	2.2(5)	
3703.6	(482.7)[d]	$7^{(-)}$	6^-	$\approx$0.2	
	632.4(5)[d]	$7^{(-)}$	(5^-)	$\approx$0.2	
	1726.0(5)	$7^{(-)}$	6^+	0.8(2)	0.4(1)
4672.9[d]	969.3(6)[d]	$9^{(-)}$	$7^{(-)}$	0.7(3)	1.1(3)
	1679.4(6)[d]	$9^{(-)}$	8^+	0.5(2)	0.4(2)
5776.1[d]	1103.2(7)[d]	(11^-)	$9^{(-)}$	0.3(1)	
6853[d]	1077(1)[d]	(13^-)	(11^-)	$\approx$0.2	
		Band 6			
2890.9[d]	1017.7(1)[d]	(4^-)	4^+	$\approx$0.5	
	1326.2(4)[d]	(4^-)	3^+	1.1(3)	
3340.6[d]	268.6(4)[d]	(6^-)	(5^-)	1.4(4)	
	276.1(5)[d]	(6^-)	5^-	6.4(23)	0.45(14)
	449.6(4)[d]	(6^-)	(4^-)	3.4(12)	
	591.6(8)[d]	(6^-)	5^-	0.3(1)	
4213.5[d]	508.6(7)[d]	(8^-)	$7^{(-)}$	0.5(2)	
	872.9(4)[d]	(8^-)	(6^-)	2.4(7)	0.85(8)
5217.3[d]	1003.8(5)[d]	(10^-)	(8^-)	3.4(6)	0.80(18)
6305[d]	1088(1)[d]	(12^-)	(10^-)	0.9(4)	
(7457)[d]	(1152)[d]	(14^-)	(12^-)	$\approx$0.4	

TABLE I. (*Continued*).

E_x(keV)[a]	E_γ(keV)	$I_i^\pi(\hbar)$	$I_f^\pi(\hbar)$	I_γ[b]	R_{DCO}[b,c]
		Band 7			
2763.5	364.4(3)[d]	4^-	3^-	1.0(2)	
	1199.1(4)	4^-	3^+	1.7(7)	0.74(23)
	1644.1(5)	4^-	4^+	4.9(13)	1.10(11)
3219.1	455.5(6)	6^-	4^-	≈6	
	470.0(5)	6^-	5^-	3.2(5)	0.4(1)
	920.1(5)	6^-	5^+	3.8(13)	0.52(4)
	1241.7(6)	6^-	6^+	2.1(8)	0.97(8)
3917.4	629.4(8)[d]	8^-	7^-	0.5(1)	
	698.3(2)	8^-	6^-	4.2(6)	1.06(7)
	715(1)	8^-	7^+	0.2(1)	0.4(1)
	924.4(7)	8^-	8^+	0.6(2)	
4807.4	890.0(3)	10^-	8^-	4.8(8)	0.83(5)
5854.0	1046.5(5)	12^-	10^-	2.2(3)	0.95(15)
7065.8	1211.8(7)	(14^-)	12^-	0.6(2)	
8468.2	1402.4(7)	(16^-)	(14^-)	0.5(2)	
10060[d]	1592(1)[d]	(18^-)	(16^-)	0.5(2)	
		Band 8			
2398.7	1943.8(4)	3^-	2^+	3.4(5)	0.41(12)
2749.1	350.5(6)	5^-	3^-	0.7(2)	0.93(6)
	771.3(6)	5^-	6^+	1.2(4)	0.4(1)
	1629.7(3)	5^-	4^+	8.9(10)	0.53(10)
3287.8	294.2(4)[d]	7^-	8^+	0.9(3)	0.49(11)
	538.9(2)	7^-	5^-	4.3(6)	1.10(12)
	1310.1(2)	7^-	6^+	5.2(4)	0.5(1)
4028.1	740.3(2)	9^-	7^-	10.3(21)	0.88(9)
	1034.7(6)	9^-	8^+	1.0(4)	0.5(1)
4965.2	937.1(4)	11^-	9^-	3.2(9)	0.96(5)
6086.4	1121.2(7)	13^-	11^-	2.4(9)	1.1(2)
7391.8	1305.3(7)	(15^-)	13^-	1.0(3)	
8881.7	1489.9(9)	(17^-)	(15^-)	0.6(3)	
10551	1669(1)	(19^-)	(17^-)	0.3(2)	
12389	1838(1)	(21^-)	(19^-)	0.3(2)	
		Additional States			
2413.0	848.4(3)		3^+	1.29(22)	
	1265.1(4)		2^+	1.44(25)	
	1293.5(4)[d]		4^+	0.55(15)	
2901.0[d]	1781.6(4)[d]		4^+	1.8(4)	
2968.5[d]	291.0(3)[d]			1.9(4)	
	569.1(3)[d]		3^-	0.5(2)	
	1403.8(7)[d]		3^+	0.7(2)	
	1820.9(6)[d]		2^+	0.4(1)	
	1849.3(6)[d]		4^+	1.6(4)	
2999.3	1851.9(6)[d]		2^+	1.13(18)	
	1879.5(6)		4^+	1.36(20)	
3036.4[d]	1917.0(5)[d]		4^+	0.75(17)	
3136.8[d]	1158.6(6)[d]		6^+	1.3(4)	
	2017.4(6)[d]		4^+	1.0(3)	
3160.4	1287.5(4)	3^-	4^+	0.6(2)	
	1595.8(5)[d]	3^-	3^+	0.8(3)	
	2012.5(6)	3^-	2^+	1.8(5)	
	2041.1(6)	3^-	4^+	1.3(3)	
3337.6[d]	338.6(3)[d]			≈0.2	
	1773.1(5)[d]		3^+	0.6(2)	
	2217.7(7)[d]		4^+	0.7(3)	
3439.9[d]	690.7(5)[d]		5^-	0.5(2)	
	1041.3(7)[d]		3^-	1.0(3)	
3548.1[d]	1248.1(5)[d]		5^+	0.2(1)	
	1570.5(6)[d]		6^+	1.0(3)	
3607.9	614.3(5)	8^+	8^+	1.6(4)	1.1(3)
	1630.4(8)	8^+	6^+	0.7(2)	

TABLE I. (*Continued*).

E_x(keV)[a]	E_γ(keV)	$I_i^\pi(\hbar)$	$I_f^\pi(\hbar)$	I_γ[b]	R_{DCO}[b,c]
3724.8	823.1(4)[d]			0.2(1)	
	1326.0(5)		3^-	0.6(2)	
	1852.4(5)		4^+	1.6(4)	
	1969.6(6)[d]		2^+	0.3(2)	
3748.1	611.3(4)[d]			≈ 0.2	
	1349.4(5)		3^-	1.5(6)	
3773.6	872.6(4)[d]	3^-		0.6(2)	
	1199.3(4)[d]	3^-		1.35(22)	
	1374.9(5)	3^-	3^-	2.7(6)	
	1901.1(6)	3^-	4^+	0.35(12)	
	2208.8(7)	3^-	3^+	0.53(18)	
3791.7[d]	653.9(7)[d]			≈ 0.2	
	1814.1(6)[d]		6^+	1.0(2)	
3919.3[d]	1520.7(6)[d]		3^-	0.8(3)	
3923.1[d]	314.8(4)[d]		8^+	1.0(3)	
	1945.8(6)[d]		6^+	0.9(3)	
4395.6	289.5(5)	10^+	10^+	0.5(2)	1.2(4)
	1402.3(6)	10^+	8^+	2.2(6)	

[a]Energy of the initial state.
[b]Determined from the ^{58}Ni(^{23}Na,3p) reaction.
[c]DCO ratios were determined from spectra gated on one or more stretched $E2$ transitions.
[d]New level assigned to ^{78}Kr or new transition placed in the level scheme.
[e]Normalization.
[f]DCO ratio of the doublet.

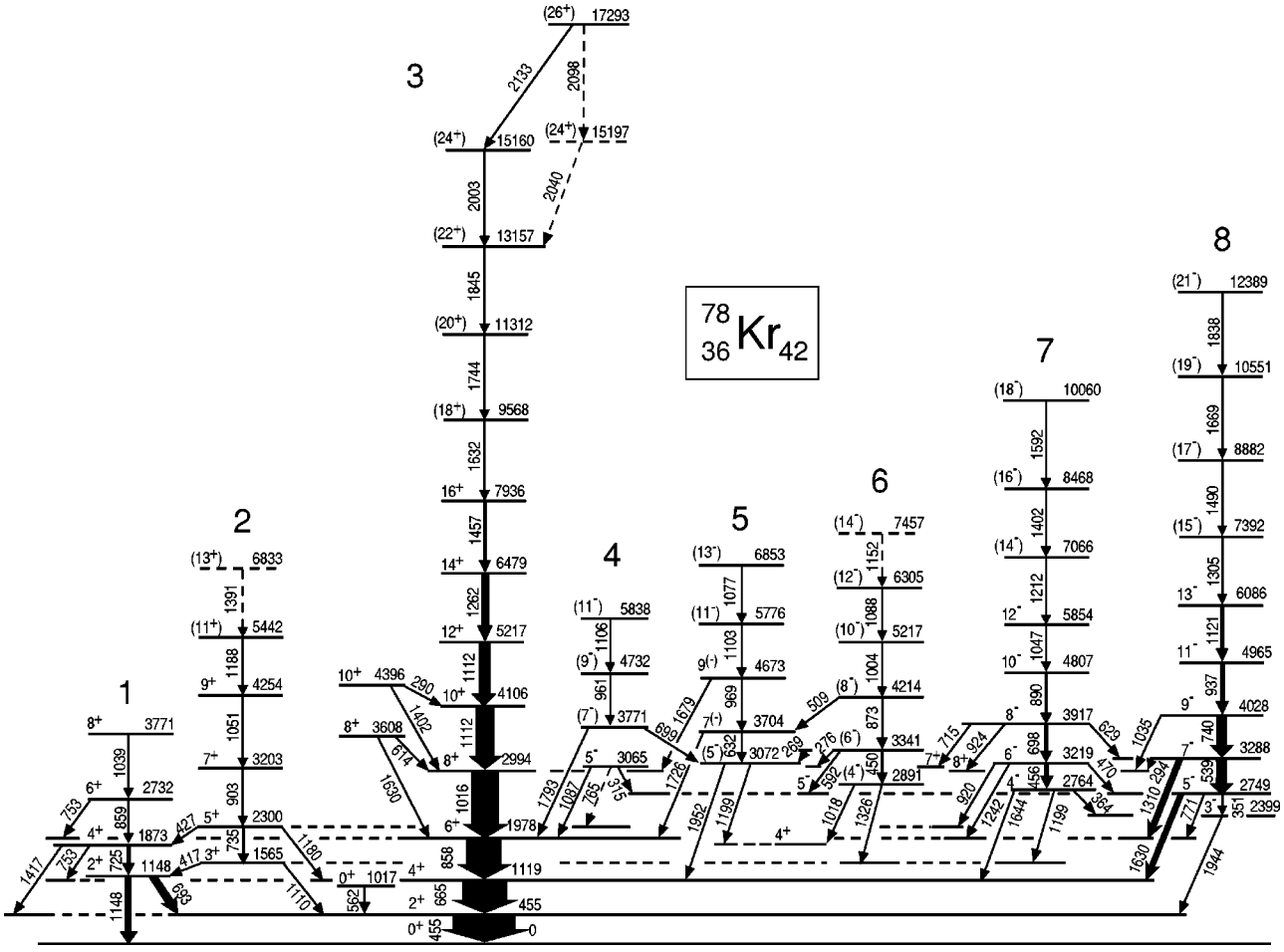

FIG. 1. The level scheme for ^{78}Kr as deduced from the present work.

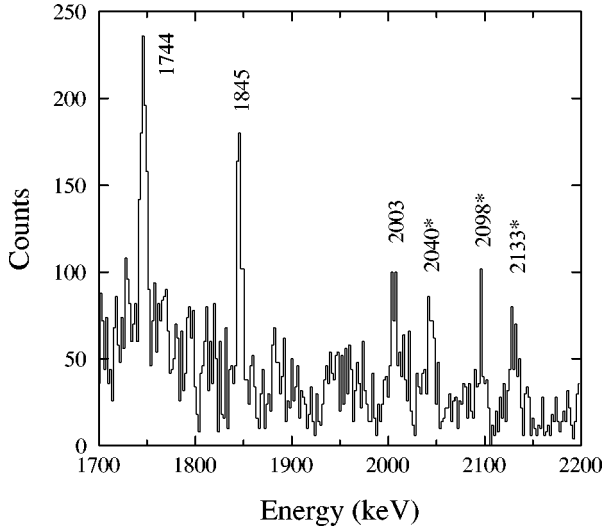

FIG. 2. A portion of the triples coincidence spectrum from the GAMMASPHERE experiment with combinations of gates on all pairs of transitions in band 3 between the 455 and 1632 keV lines. Newly reported lines are indicated with asterisks.

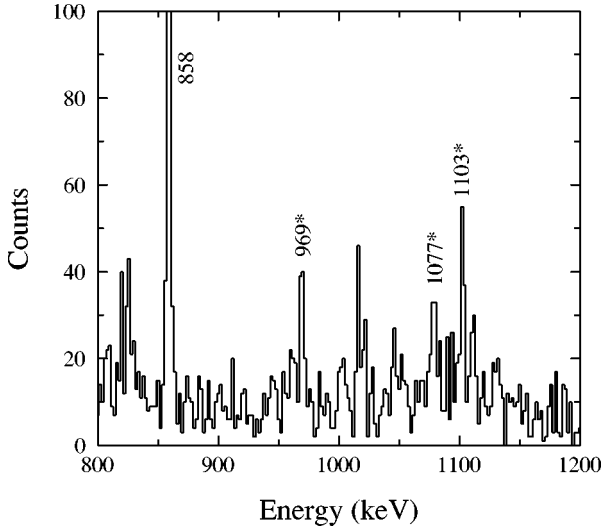

FIG. 4. A portion of the spectrum in coincidence with either the 969 or the 1726 keV lines in band 5 observed in the ^{58}Ni(^{23}Na,3p) reaction. New transitions assigned to ^{78}Kr are indicated with asterisks.

D. Negative-parity bands 7 and 8

One pair of signature-partner negative-parity bands was known in ^{78}Kr from prior work [7,12]. The odd-spin sequence, band 8, is built on the low-lying 3^- level at 2399 keV and was identified up to a tentative (21^-) state at 12389 keV. The even-spin sequence, band 7, starts at the 2764 keV 4^- level and was observed in prior work [7] through a 16^- level at 8469 keV. A transition of 1592 keV was seen in the GAMMASPHERE data, extending this sequence up to the (18^-) state at 10 060 keV. Additional decay lines of 294, 364, and 629 keV were seen from these bands. The measured DCO ratios permitted firm spin assignments to several additional states in the two bands.

E. Additional states

Additional yrare 8^+ and 10^+ states decaying into the yrast band were previously reported [10,11,13]. These states have been confirmed in the present work. The present excitation energies of 3608 and 4396 keV are within 1 keV of the previously reported values, except for a value about 9 keV lower reported in Ref. [10] for the 8^+ state. Two decay branches have been observed from this state in the present work, in agreement with an earlier report [13]. The 3608 keV level was first assigned a spin-parity of 7^- in Ref. [13] and later (8^+) in Refs. [10,11]. The present assignment of 8^+ agrees with the latter one and is based on the DCO ratio of the 614 keV transition and the existence of the 1630 keV decay.

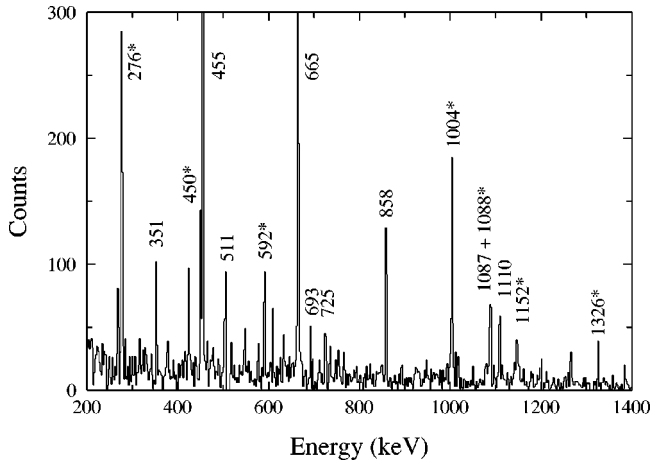

FIG. 3. A portion of the γ spectrum in coincidence with the 873 keV line in band 6 as observed in the ^{58}Ni(^{23}Na,3p) reaction. New transitions assigned to ^{78}Kr in the present work are indicated with asterisks.

The ^{23}Na+^{58}Ni reaction also populated ^{78}Rb strongly [22]. Therefore some of the states observed in ^{78}Kr in the FSU data were populated following the β decay of the 4^- isomer and (to a lesser extent) the 0^+ ground state of ^{78}Rb [25–27]. States for which new information was obtained are listed in Table I, but not shown in Fig. 1. Since the initial alignment is lost before β decay occurs, DCO ratios are not meaningful for γ transitions in the daughter nucleus.

The second 0^+ state at 1017 keV is shown on the level scheme since its 562 keV decay transition was clearly seen in the data. No connections could be reliably established with any states in Fig. 1 above the 2_1^+ level. Coincidences were seen between the 562 keV line and γ rays of 738 and 2420 keV, confirming some previous β-decay results [25–27].

IV. DISCUSSION

A. Positive-parity bands

The kinematic moments of inertia $J^{(1)}$ in bands 1–3 are compared in the lower part of Fig. 5. For the yrast band 3, $J^{(1)}$ generally increases over the observed spin range from $0\hbar$ to $26\hbar$. The irregularities at rotational frequencies $\hbar\omega$ of 0.55 and 0.9 MeV have previously been associated with $g_{9/2}$ pair alignments. There has been some difficulty in determining which alignment is associated with $g_{9/2}$ protons and which with $g_{9/2}$ neutrons, in part because protons and neutrons in ^{78}Kr occupy the same major shell. Hartree-Fock-

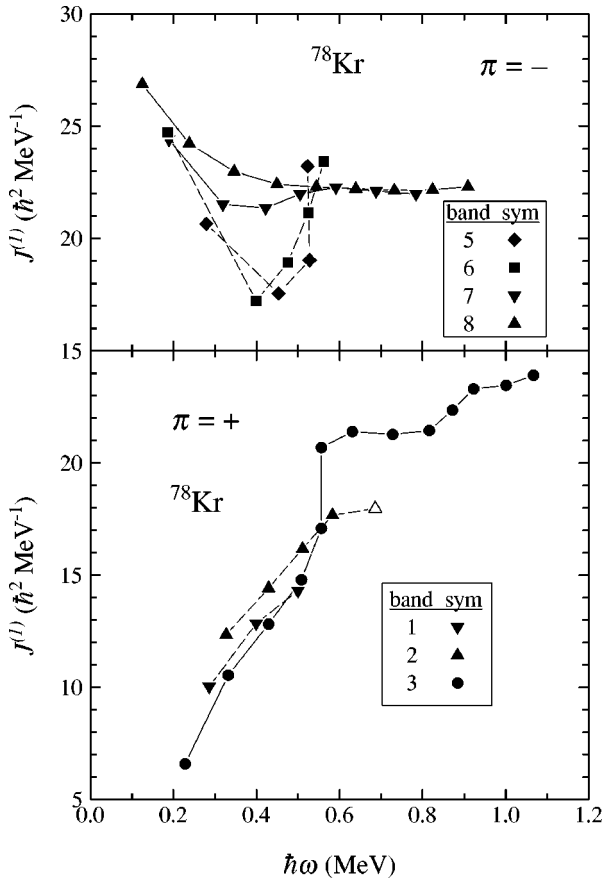

FIG. 5. Kinematic moments of inertia $J^{(1)}$ calculated for the bands in ^{78}Kr. The following list gives the band numbers followed by the K value used in parenthesis: 1–2 ($K=2$), 3($K=0$), 5–8 ($K=3$).

Bogoliubov (HFB) cranking calculations [7] predict a well-deformed, but γ-soft, shape with two energy minima for the low-energy states of ^{78}Kr. It was first suggested [7] that the yrast band corresponds to the triaxial minimum ($\beta_2 \approx 0.3$, $\gamma \approx -15°$). This accounts nicely for the first crossing as a proton alignment, but predicts the second, neutron, alignment too low in frequency (0.6 MeV$\leqslant \hbar\omega \leqslant$0.7 MeV). A subsequent g-factor measurement reported [14] that the observed rotation implies a g factor significantly less than the collective value for the 8^+ state or for states just above it. This was interpreted as a strong indication that the first crossing is a neutron alignment and that the yrast band corresponds to the nearly oblate minimum in the HFB calculations. The configuration-dependent shell-correction calculations discussed in Sec. IV B also predict an oblate shape around spin 8, in confirmation of this interpretation.

A neutron $g_{9/2}$ crossing at the 8^+ state has been deduced from recent deformed configuration mixing (DCM) shell-model calculations [9]. This differs from the HFB results because the neutron crossing occurs at prolate ($\beta_2 \approx 0.21$), rather than oblate, shape. The DCM calculations also predict a proton $g_{9/2}$ crossing at the 14^+ state. One difference between the DCM and HFB calculations is that the fp orbitals are grouped about a factor of two closer together in the DCM, giving rise to a much larger gap at particle number 40.

Comparisons with neighboring nuclei are not as helpful in this mass region because of the rapid shape changes which can occur with small changes in particle numbers. The proton and neutron alignments are nearly simultaneous in ^{76}Kr [7,12], where the predicted prolate shape appears to be consistent with the observed data. On the other hand, only one alignment has been observed in ^{80}Kr up to $\hbar\omega = 0.9$ MeV [16]. HFB calculations predict an oblate shape which would imply that the neutrons align first. However, there are no g-factor measurements or other direct evidence to determine the nature of the alignment in ^{80}Kr. Earlier interpretations favored a proton alignment. It appears likely that the shape of the yrast band in the even-even Kr isotopes changes from prolate in ^{76}Kr to oblate in ^{80}Kr.

The other positive-parity bands are energetically unfavored and more difficult to explore experimentally. Two $\Delta I = 1$ decays between bands 2 and 1 and the relative positions of the states suggest that bands 1 and 2 may be signature partners. The moments of inertia of these two bands follow that of the yrast band rather closely except for the last point where two-quasiparticle configurations become important. Reasonably good agreement was obtained between the properties of these bands and the γ-bands predicted in interacting neutron-proton boson model calculations [5].

The 8^+ and 10^+ states at 3608 and 4396 keV look similar to a pair of states of the same spin reported in ^{80}Kr [16], and no connecting $E2$ transition was observed. A two-level mixing calculation was performed to infer the unperturbed energies of the corresponding yrast states in ^{78}Kr [10] and account for irregularities in the band structures. The difference of about 9 keV in the position of the 8^+ state between Ref. [10] and the present work does change the conclusions of that study.

B. Configuration-dependent shell-correction calculations

To understand the forking seen at the top of band 3 and further examine the shape of this band, calculations have been performed within the configuration-dependent shell-correction approach with the cranked Nilsson potential using parameters previously fitted to $A \approx 80$ nuclei [28], as described in Refs. [29–31]. Pairing correlations have been neglected, so the predicted energies can be considered realistic for spins above 10 or 15$\hbar$. The full Nilsson Hamiltonian has been diagonalized in the calculations, even though the configurations will be discussed below in terms of the main components of their wave functions.

The calculated energies of the lowest positive-parity, even-spin configurations are shown in Fig. 6 after subtraction of the energies of a rigid rotor to magnify the deviations from rigid rotation. The measured energies of band 3 (above the region where pairing is most important) are shown in the same way in the figure for comparison. The theoretical curves are labeled by their dominant configurations according to [$p1$,$n1$], where $p1(n1)$ is the number of protons (neutrons) in the $g_{9/2}$ orbital.

The [2,4] configuration forms the lowest collective band below spin 24$\hbar$. The shape of this curve is rather similar to the experimental data over the range $10 \leqslant I \leqslant 24$. The good agreement above spin 10$\hbar$ is similar to what has been seen for ^{81}Sr [32] and gives additional confidence in other predictions of the model. No real termination is seen for the calculated [2,4] configuration because the proton holes migrate

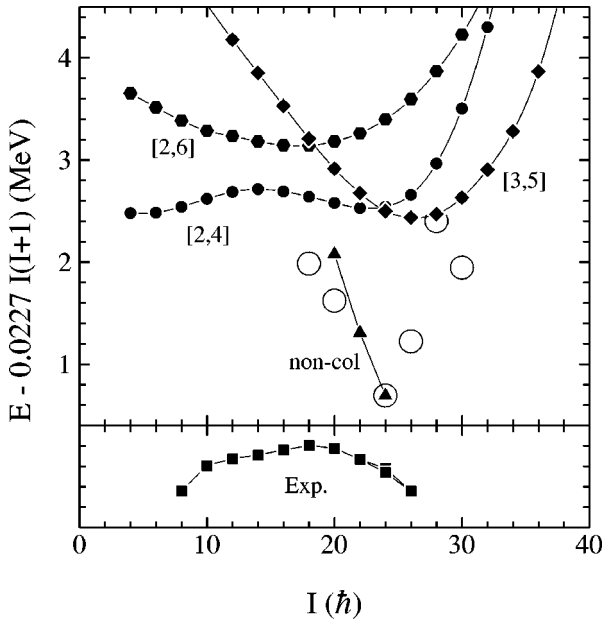

FIG. 6. Energies relative to a rigid rotor calculated within the configuration-dependent shell-correction approach with a cranked Nilsson potential. The labeling of the theoretical curves is discussed in the text. The observed level energies in band 3 relative to the same rotor are shown with squares in the lower panel. The experimental curve is graphed with the same dispersion but its absolute position relative to the theoretical ones is arbitrary.

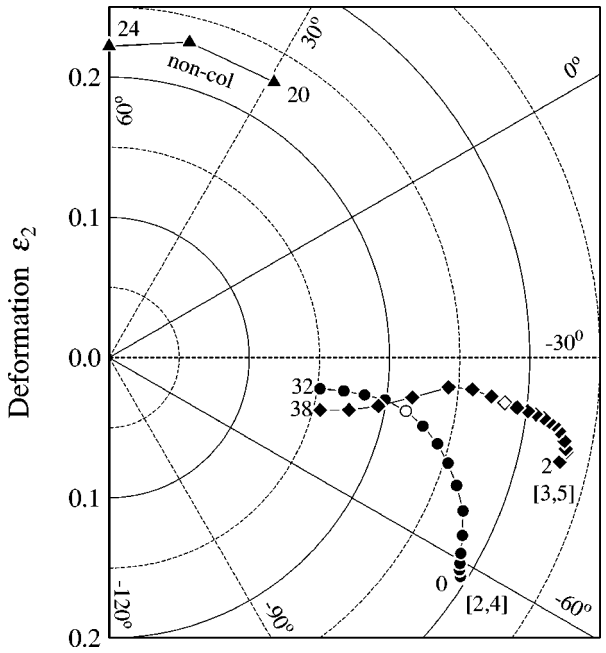

FIG. 7. Evolution of predicted shape with spin for 3 configurations calculated in the configuration-dependent shell-correction approach. The shapes are shown on a polar graph with the magnitude of quadrupole deformation ϵ_2 as the radial coordinate and the triaxiality parameter γ as the angular one. Lines of constant γ are drawn at 30° intervals. The starting and ending spins are indicated for each sequence. Since a number of the low-spin points overlap, the shapes at the crossing point, $24\hbar$, are shown with open symbols.

down to the $f_{7/2}$ subshell. The result is a steady rise in energy relative to the rigid rotor value above spin $22\hbar$. A well-deformed, oblate shape ($\epsilon_2=0.29$, $\gamma=-60°$) is predicted for this configuration up to spin $12\hbar$, as shown in Fig. 7. As mentioned in the last section, this prediction of oblate shape agrees well with the neutron alignment observed in the *g*-factor measurement. Above $12\hbar$, ϵ_2 decreases and the shape becomes more triaxial. Because no true termination occurs, γ does not reach $+60°$.

Although the more deformed [3,5] configuration lies considerably higher at low spins, it falls rapidly with spin and is predicted to cross the [2,4] configuration at spin $24\hbar$. This is exactly the point at which a forking is observed in band 3 and suggests that the observed forking may result from a crossing of the calculated [2,4] and [3,5] bands. If so, the agreement is remarkably good, although perhaps somewhat less surprising in view of the good agreement observed earlier in ^{81}Sr [32]. In this interpretation, the last 26^+ state seen experimentally would correspond to the [3,5] configuration and the next state would be harder to observe because the theoretical curve is starting to rise at $28\hbar$. The predicted deformation for this configuration (see Fig. 7) starts at $\epsilon_2=0.33$ and decreases steadily with spin while γ remains about $-40°$.

The [2,6] configuration is predicted to be somewhat more deformed ($\epsilon_2=0.36$), but would be more difficult to observe since it always lies above the [2,4] and [3,5] configurations. Other interesting predictions of the model which have not yet been seen experimentally are the yrast noncollective states. They are indicated mostly with large open circles in Fig. 6. A very short terminating band consisting of only the $I=20-24$ states can be identified in the calculations. The main difference between the collective and noncollective configurations in the calculations appears to be that both the $p_{1/2}$ proton and neutron holes couple to spin 0 in the latter case. By contrast, no pair of $N=3$ holes couples to spin 0 among the collective configurations. One could also note that the more collective bands are generally located ''below'' the $\gamma=-30°$ line in Fig. 7, while the states with little or no collectivity lie near $+60°$ with $\epsilon_2\sim0.20-0.25$. Rather similar noncollective yrast states appeared in the ^{81}Sr calculations [32] and also await experimental observation.

C. Negative-parity bands

In contrast to those in the positive-parity bands, the moments of inertia in the two previously known negative-parity bands 7 and 8 start at higher values and drop to reach a remarkably constant value of 22 to 23 $\hbar^2$/MeV (see Fig. 5). Although they begin from very different values, the moments of inertia in the bands of both parities converge to similar values (approximately the rigid-rotor value) at the highest rotational frequencies, most likely due to the decreasing influence of pairing [33]. The behavior of the $J^{(1)}$ values in bands 7 and 8 is rather similar to that of the lowest negative-parity bands in ^{76}Kr [15] except that no evidence is seen for an alignment in ^{78}Kr up to $\hbar\omega=0.9$ MeV, whereas a clear alignment was seen in ^{76}Kr at $\hbar\omega\approx0.8$ MeV.

In ^{74,76,78}Kr the lowest negative-parity bands were associated with the two-quasiproton configuration $\pi[431]^{\frac{3}{2}+}\otimes\pi[312]^{\frac{3}{2}-}$, based in large part on the absence of a lower frequency proton alignment expected for a two-quasineutron

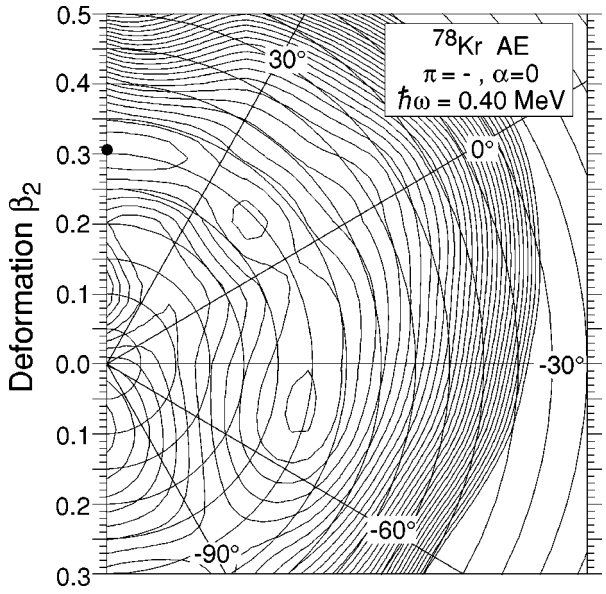

FIG. 8. Total Routhian surface for the two-quasineutron configuration AE corresponding to a negative-parity, even-spin band at a rotational frequency of $\hbar\omega = 0.40$ MeV. The spacing between contour lines is 0.25 MeV.

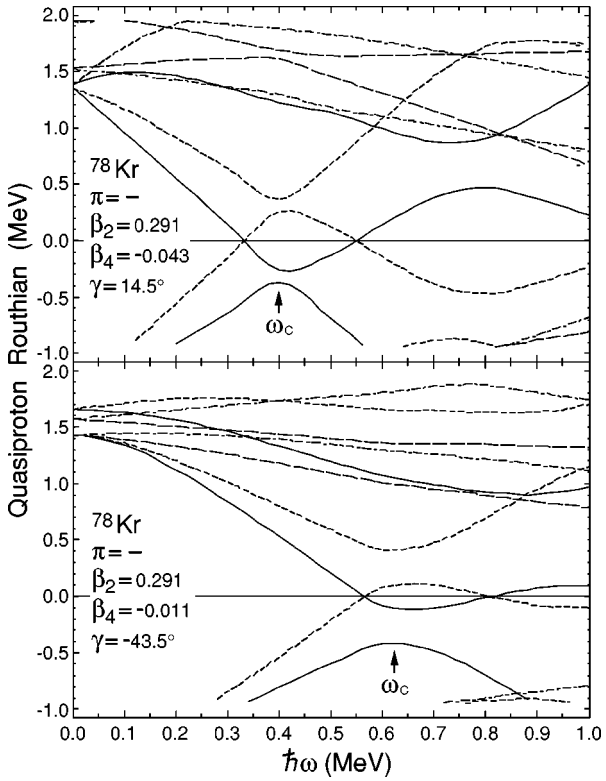

FIG. 9. Single quasiproton energies as a function of rotational frequency for the indicated shapes. Parity and signature (π,α) of the Routhians are indicated in the following way: $(+,\frac{1}{2})$, solid line; $(+,-\frac{1}{2})$, dotted line; $(-,\frac{1}{2})$, dash-dotted line; $(-,-\frac{1}{2})$, dashed line.

configuration [3,7]. This analysis was confirmed nicely when a higher-lying pair of negative-parity bands was found in ^{76}Kr, which do align at a much lower frequency [15]. They are the two-quasineutron bands. Measurements of g factors in bands 7 and 8 of ^{78}Kr showed precession angles significantly larger than in the yrast band [14]. This was interpreted as strong evidence for the two-quasiproton nature of these bands. The DCM calculations [9] also predict a signature-partner pair of negative-parity bands at about the energies seen experimentally, although an inversion occurs at the bottom of the band with the 3^- level above the 5^- one. These bands also involve a two-quasiproton configuration, in agreement with the HFB results.

The moments of inertia for new bands 5 and 6 differ significantly from those of bands 7 and 8 by increasing rapidly with frequency above $\hbar\omega > 0.45$ MeV. This behavior is very similar to what was seen in the new negative-parity bands in ^{76}Kr and indicates at least the start of a quasiparticle alignment at $0.45\ \text{MeV} \leqslant \hbar\omega \leqslant 0.55$ MeV. The analogy with ^{76}Kr suggests that bands 5 and 6 may have a two-quasineutron configuration. Also, only one energy minimum appears in the total Routhian surface (TRS) shown in Fig. 19 of Ref. [7] for the two-quasiproton configuration of signature $\alpha = 0$, $r = +1$ (even spins), and this was assigned to band 7.

HFB calculations were examined for the lowest two-quasineutron configuration with signature $\alpha = 0$ (even spins), usually designated the AE configuration [34]. The resulting TRS at a rotational frequency of $\hbar\omega = 0.4$ MeV, shown in Fig. 8, implies a substantial quadrupole deformation of $\beta_2 \approx 0.3$, but a wide range of possible γ values. Three energy minima occur at (β_2,γ) values of $(0.31,\ +60°)$, $(0.29,\ +15°)$, and $(0.29,\ -44°)$, but configurations at intermediate γ values are hardly less favored. A shape at or near the noncollective value of $\gamma = 60°$ is very unlikely to correspond to the observed band. Because one of the quasineutrons in this configuration lies in a $g_{9/2}$ orbital, Pauli blocking arguments imply that the lowest alignment should be among the $g_{9/2}$ quasiprotons. The single quasiproton energies are shown as a function of rotational frequency in Fig. 9 for both the nearly prolate shape of $\gamma = +15°$ and the nearly oblate shape of $\gamma = -44°$. The predicted proton alignment frequencies of $\hbar\omega = 0.4$ and 0.65 MeV, respectively, bracket the observed value. Thus, a two-quasineutron configuration with a predicted β_2 of 0.29 and a γ value intermediate between the two minima in Fig. 8 would be consistent with the observed bands 5 and 6. This is quite reasonable, given the γ softness of the TRS.

V. SUMMARY

High-spin states in ^{78}Kr were examined using the ^{58}Ni(^{23}Na,3p) reaction at 70 MeV and the ^{58}Ni(^{28}Si,$\alpha 4p$) reaction at 130 MeV. Prompt γ-γ coincidences were measured using the Pitt-FSU detector array and the GAMMASPHERE-MICROBALL array. A number of new transitions and energy levels were found, and spin assignments were made using DCO ratios. Three new bands were identified. On the basis of the observed alignment and HFB calculations, two of them appear to be based on a two-quasineutron structure, complementing the previously known two-quasiproton band. This extends a pattern of parallel proton and neutron excitations that was first seen in ^{76}Kr.

An interesting forking behavior has been observed at the top of the yrast band. Configuration-dependent shell-correction calculations interpret this forking as an unpaired crossing of the [2,4] ground band by the more deformed [3,5] structure at spin $24\hbar$. Across the even Kr isotopes, the

shape of the yrast band appears to change from prolate for ^{74,76}Kr to oblate for ^{80}Kr. Although earlier HFB calculations suggested a prolate shape for ^{78}Kr, an oblate shape is required to reproduce the first neutron crossing implied by *g*-factor measurements. The configuration-dependent shell-correction calculations, which account nicely for the observed forking at high spins, predict an oblate shape at low to moderate spins, in agreement with the *g*-factors. The bulk of the available evidence now favors an oblate shape for the yrast band, but more prolate shapes for the negative-parity bands. This would imply that prolate and oblate shapes coexist in ^{78}Kr.

ACKNOWLEDGMENTS

We are grateful to Dr. W. Nazarewicz for providing his Hartree-Fock-Bogoliubov cranking computer codes. This work was supported in part by the U.S. National Science Foundation, the U.S. Department of Energy, and the Swedish Natural Science Council.

[1] S. L. Tabor, P. D. Cottle, J. W. Holcomb, T. D. Johnson, P. C. Womble, S. G. Buccino, and F. E. Durham, Phys. Rev. C **41**, 2658 (1990).

[2] J. Heese, D. J. Blumenthal, A. A. Chishti, P. Chowdhury, B. Crowell, P. J. Ennis, C. J. Lister, and Ch. Winter, Phys. Rev. C **43**, R921 (1991).

[3] D. Rudolph, C. Baktash, C. J. Gross, W. Satula, R. Wyss, I. Birriel, M. Devlin, H.-Q. Jin, D. R. LaFosse, F. Lerma, J. X. Saladin, D. G. Sarantites, G. N. Sylvan, S. L. Tabor, D. F. Winchell, V. Q. Wood, and C. H. Yu, Phys. Rev. C **56**, 98 (1997).

[4] P. Kemnitz, P. Ojeda, J. Döring, L. Funke, L. K. Kostov, H. Rotter, E. Will, and G. Winter, Nucl. Phys. **A425**, 493 (1984).

[5] H. P. Hellmeister, J. Keinonen, K. P. Lieb, U. Kaup, R. Rascher, R. Ballini, J. Delaunay, and H. Dumont, Nucl. Phys. **A332**, 241 (1979); Phys. Lett. **85B**, 34 (1979).

[6] R. Soundranayagam, S. Ramavataram, A. V. Ramayya, J. H. Hamilton, and R. L. Robinson, Phys. Rev. C **25**, 2983 (1982).

[7] C. J. Gross, J. Heese, K. P. Lieb, S. Ulbig, W. Nazarewicz, C. J. Lister, B. J. Varley, J. Billowes, A. A. Chishti, J. H. McNeill, and W. Gelletly, Nucl. Phys. **A501**, 367 (1989).

[8] W. Nazarewicz, J. Dudek, R. Bengtsson, T. Bengtsson, and I. Ragnarsson, Nucl. Phys. **A435**, 397 (1985).

[9] K. C. Tripathy and R. Sahu, Nucl. Phys. **A597**, 177 (1996).

[10] G. Winter, F. Dubbers, J. Döring, L. Funke, P. Kemnitz, E. Will, D. S. Andreev, K. I. Erochina, I. Kh. Lemberg, A. A. Pasternak, L. A. Rassadin, and I. N. Chugunov, J. Phys. G **11**, 277 (1985).

[11] D. S. Andreev, K. I. Erokhina, I. Kh. Lemberg, A. A. Pasternak, L. A. Rassadin, and I. N. Chugunov, Izv. Akad. Nauk SSSR, Ser. Fiz. **46**, 22 (1982).

[12] M. S. Kaplan, J. X. Saladin, L. Faro, D. F. Winchell, H. Takai, and C. N. Knott, Phys. Lett. B **215**, 251 (1988).

[13] R. L. Robinson, H. J. Kim, R. O. Sayer, W. T. Milner, R. B. Piercey, J. H. Hamilton, A. V. Ramayya, J. C. Wells, Jr., and A. J. Caffrey, Phys. Rev. C **21**, 603 (1980).

[14] J. Billowes, F. Cristancho, H. Grawe, C. J. Gross, J. Heese, A. W. Mountford, and M. Weiszflog, Phys. Rev. C **47**, R917 (1993).

[15] J. Döring, G. D. Johns, R. A. Kaye, M. A. Riley, S. L. Tabor, P. C. Womble, and J. X. Saladin, Phys. Rev. C **52**, R2284 (1995).

[16] J. Döring, V. A. Wood, J. W. Holcomb, G. D. Johns, T. D. Johnson, M. A. Riley, G. N. Sylvan, P. C. Womble, and S. L. Tabor, Phys. Rev. C **52**, 76 (1995).

[17] S. L. Tabor, M. A. Riley, J. Döring, P. D. Cottle, R. Books, T. Glasmacher, J. W. Holcomb, J. Hutchins, G. D. Johns, T. D. Johnson, T. Petters, O. Tekyi-Mensah, P. C. Womble, L. Wright, and J. X. Saladin, Nucl. Instrum. Methods Phys. Res. B **79**, 821 (1993).

[18] S. L. Tabor, Nucl. Instrum. Methods Phys. Res. A **265**, 495 (1988).

[19] I. Y. Lee, Nucl. Phys. **A520**, 641c (1990).

[20] D. G. Sarantites, P.-F. Hua, M. Devlin, L. G. Sobotka, J. Elson, J. T. Hood, D. R. LaFosse, J. E. Sarantites, and M. R. Maier, Nucl. Instrum. Methods Phys. Res. A **381**, 418 (1996).

[21] E. F. Moore, P. D. Cottle, C. J. Gross, D. M. Headly, U. J. Hüttmeier, S. L. Tabor, and W. Nazarewicz, Phys. Rev. C **38**, 696 (1988).

[22] R. A. Kaye, J. Döring, J. W. Holcomb, G. D. Johns, T. D. Johnson, M. A. Riley, G. N. Sylvan, P. C. Womble, V. A. Wood, S. L. Tabor, and J. X. Saladin, Phys. Rev. C **54**, 1038 (1996).

[23] G. N. Sylvan, J. Döring, G. D. Johns, S. L. Tabor, C. J. Gross, C. Baktash, H.-Q. Jin, D. W. Stracener, P. F. Hua, M. Korolija, D. R. LaFosse, D. G. Sarantites, F. Cristancho, E. Landulfo, J. X. Saladin, B. Cederwall, I. Y. Lee, A. O. Macciavelli, W. Rathbun, and A. Vander Molen, Phys. Rev. C **56**, 772 (1997).

[24] C. J. Gross, C. Baktash, D. M. Cullen, R. A. Cunningham, J. D. Garrett, W. Gelletly, F. Hannachi, A. Harder, M. K. Kabadiyski, K. P. Lieb, C. J. Lister, W. Nazarewicz, H. A. Roth, D. Rudolph, D. G. Sarantites, J. A. Sheikh, J. Simpson, Ö. Skeppstedt, B. J. Varley, and D. D. Warner, Phys. Rev. C **49**, R580 (1994).

[25] A. Giannatiempo, A. Nannini, A. Perego, P. Sona, M. J. G. Borge, O. Tenglbad, and the ISOLDE Collaboration, Phys. Rev. C **52**, 2444 (1995).

[26] G. K. Bavaria, J. E. Crawford, S. Calamawy, and J. E. Kitching, Z. Phys. A **302**, 329 (1981).

[27] E. Nolte and Y. Shida, Z. Phys. **256**, 243 (1972).

[28] D. Galeriu, D. Bucurescu, and M. Ivaşcu, J. Phys. G **12**, 329 (1986).

[29] T. Bengtsson and I. Ragnarsson, Nucl. Phys. **A436**, 14 (1985).

[30] I. Ragnarsson, V. P. Janzen, D. B. Fossan, N. C. Schmeing, and R. Wadsworth, Phys. Rev. Lett. **74**, 3935 (1995).

[31] A. V. Afanasjev and I. Ragnarsson, Nucl. Phys. **A591**, 387 (1995).

[32] I. Ragnarsson and A. V. Afanasjev, in Proceedings of the Conference on Nuclear Structure at the Limits, Argonne, 1996, Report No. ANL-PHY-97/1, p. 184.

[33] S. L. Tabor, Phys. Rev. C **45**, 242 (1992).

[34] R. Wyss, F. Lidén, J. Nyberg, A. Johnson, D. J. G. Love, A. H. Nelson, D. W. Banes, J. Simpson, A. Kirwan, and R. Bengtsson, Nucl. Phys. **A503**, 244 (1989).